Title

Numerical analysis of coupled wedge plasmons in a structure of two metal wedges separated by a gap

Journal

Journal of Applied Physics, 100(1)

ISSN

0021-8979

Authors

Pile, DFP
Gramotnev, Dmitri K
Haraguchi, M
et al.

Publication Date

2006-07-01

Peer reviewed

Numerical analysis of coupled wedge plasmons in a structure of two metal wedges separated by a gap

D. F. P. Pile[a)]
Department of Optical Science and Technology, Faculty of Engineering, The University of Tokushima, Minamijosanjima 2-1, Tokushima 770-8506, Japan

D. K. Gramotnev[b)]
Applied Optics Program, School of Physical and Chemical Sciences, Queensland University of Technology, GPO Box 2434, Brisbane, QLD 4001, Australia

M. Haraguchi, T. Okamoto, and M. Fukui
Department of Optical Science and Technology, Faculty of Engineering, The University of Tokushima, Minamijosanjima 2-1, Tokushima 770-8506, Japan

(Received 1 February 2006; accepted 11 April 2006; published online 5 July 2006)

This paper presents the results of the numerical finite-difference time-domain analysis of a strongly localized antisymmetric plasmon, coupled across a nanogap between two identical metal wedges. Dispersion, dissipation, field structure, and existence conditions of such coupled wedge plasmons are determined and investigated on an example of the fundamental coupled mode. It is shown that in the general case there exist three critical wedge angles and a critical gap width (separation between the wedge tips). If the gap width is larger than the critical separation, then the antisymmetric wedge plasmons can exist only in the ranges between the first and the second critical angles, and between the third critical angle and 180°. If the gap width is smaller or equal to the critical separation, then the third and the second critical angles merge, leaving only one interval of wedge angles within which the antisymmetric coupled wedge plasmons can exist. The effect of rounded wedge tips is also investigated and is shown to be similar to that of different wedge angles. Feasibility of using these plasmons for the design of efficient subwavelength waveguides is discussed. © *2006 American Institute of Physics*. [DOI: 10.1063/1.2208291]

I. INTRODUCTION

Modern microelectronics is rapidly approaching its limit in terms of speed and efficiency of information processing. Therefore, alternative means for sustainable advancement of computer technology, information processing, and storage are urgently required. One of such alternatives is related to using light as an information carrier in integrated circuits and devices. This means replacing conventional electronic devices and circuits by much more efficient optical counterparts.

However, conventional optical devices and interconnectors using dielectric waveguides and structures suffer from a significant drawback. This is the diffraction limit of light,[1–3] which means that electromagnetic waves cannot be localized (focused) within a region with dimensions that are much smaller than the wavelength in the structure. This is the major obstacle on the way of achieving high degree of miniaturization and integration of optical devices and circuits. The main approach to overcome this problem is related to use of surface plasmons in metallic nanostructures, such as rectangular metallic nanostrips,[4,5] nanorods,[3,6] nanochains,[1,2,7] metallic gaps,[8–12] metallic nanogrooves,[13–18] and nanowedges.[19–21]

All these structures are capable of guiding special types of plasmonic eigenmodes that are characterized by strong localization beyond the diffraction limit. However, different metallic nanostructures may provide different options and possibilities in terms of design of efficient subwavelength optical waveguides, interconnectors, and devices. For example, it has also been demonstrated that strongly localized plasmons in nanogrooves and nanogaps are of most interest for the development of nano-optical structures and circuits. This is because of their relatively low dissipation,[14,15] low sensitivity to structural imperfections,[17] possibility of nearly 100% transmission through sharp bends,[16] strong subwavelength localization,[14,15] etc.

In particular, the analysis of guided modes in a plasmonic waveguide in the form of a nanogap in a thin metal film/membrane has revealed that the fundamental mode guided by the gap is characterized by an unusual dependence of its dispersion on thickness of the metal film.[12] This is because the fundamental mode of the gap plasmon waveguide can be represented by four coupled wedge plasmons propagating along the edges of the gap.[12] Therefore, detailed investigation of coupled wedge plasmons is important for understanding of the behavior of strongly localized modes in gap plasmon waveguides. In addition, strongly localized plasmons propagating in a structure of two coupled wedges can themselves provide interesting options for the design of subwavelength optical components. The analysis of coupled wedge plasmons is also expected to provide an important

[a)]Present address: 5130 Etcheverry Hall, NSF Nanoscale Science and Engineering Center, University of California, Berkeley, California 94720-1740; electronic mail: d.pile@berkeley.edu
[b)]electronic mail: d.gramotnev@qut.edu.au

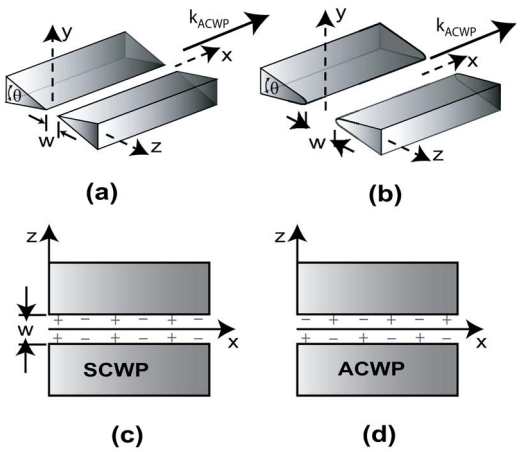

FIG. 1. Structures with two identical coupled wedges in vacuum: (a) triangular wedges with sharp tips, (b) wedges with rounded tips of radii r. The width of the gap is w, the wedge angles are θ. (c) and (d) Schematic distributions of charges across the gap in symmetric (c) and antisymmetric (d) coupled wedge plasmons. k_{ACWP} is the wave vector of the antisymmetric coupled wedge plasmon.

physical insight and better understanding of propagation and the existence conditions of strongly localized modes in wedgelike structures.

Therefore, the aim of this paper is in numerical analysis of strongly localized wedge plasmons propagating in two identical metallic wedges, coupled across a nanogap and characterized by the antisymmetric distribution of charges across the gap. Dispersion, dissipation, field structure, and existence conditions of such antisymmetric coupled wedge plasmons (ACWPs) will be determined and analyzed. The dependencies of the ACWP properties on wedge angle, separation between the tips, and radius of curvature of the rounded tips will be determined and investigated in detail on the example of the fundamental ACWP mode propagating in the structure. Possibilities of using ACWPs for the design of efficient subwavelength waveguides and interconnectors are also discussed.

II. STRUCTURE AND METHODS OF ANALYSIS

The analyzed structure consists of two identical wedges separated by a nanogap—1(a). The tips of the wedges can be either triangular [Fig. 1(a)], or rounded with the radius of curvature r [Fig. 1(b)]. Here, we will consider only the situations where the curved surface of a rounded tip is connected smoothly with the flat sides of the wedge (without additional corners between the rounded tip and the flat sides of the wedge)—Fig. 1(b). The width of the gap between the two wedges is w and the angle of the wedges is θ [Figs. 1(a) and 1(b)]. The system of coordinates is presented in Figs. 1(a) and 1(b) with the origin being in the middle of the gap between the wedges. The wedges are made of silver and surrounded by vacuum. The coupled wedge plasmons propagate in the positive x direction.

The numerical analysis of the Maxwell equations in the considered structures is carried out by means of the compact two-dimensional (compact-2D) finite-difference time-domain (FDTD) algorithm.[22] The artificial absorbing boundary conditions of the first-order Mur-type are used at the edges of the computational window.[23]

The numerical algorithm assumes that the structure is infinitely long along the x axis. The plasmons are excited by introducing a generating pulse near the wedges.[21,22] This pulse is represented by some electromagnetic field with arbitrarily selected distribution in the (y,z) plane, but periodic (with some preselected period λ) along the x axis. The generating pulse is assumed to be switched on for a period of time Δt. If the time interval Δt is sufficiently short, then the generating pulse contains a wide range of frequencies. If we allow the field to evolve in time beyond the time interval Δt, then only the frequencies corresponding to the structural eigenmodes will remain. The field intensities at the frequencies that do not correspond to the structural eigenmodes will correspond to exponentially decaying (in time) fields. Therefore, if we allow the system to evolve for a sufficiently long period of time beyond the generating pulse, the field distribution evolves to that corresponding to the interference pattern of the possible structural eigenmodes.[22] The Fourier analysis of this pattern[22] gives different frequencies of the eigenmodes, such that the wavelengths of all these eigenmodes are the same and equal to λ—the spatial period of the generating pulse. Thus the dispersion of different structural eigenmodes are determined using the compact-2D FDTD.[22] Adjusting the central frequency of the generating pulse, so that it equals the frequency of one of the eigenmodes, and increasing the length of the pulse Δt, so that the frequency band in the pulse is reduced to exclude all other modes, we obtain the field distribution, dispersion, and dissipation of a particular selected eigenmode. This is how separate eigenmodes in a multimode guiding structure can be investigated.

The described compact-2D FDTD analysis showed that there exist numerical solutions to the Maxwell equations, representing the electromagnetic fields strongly localized near the tips of the coupled wedges [Figs. 1(a) and 1(b)]. These solutions correspond to two wedge plasmons[21] traveling along the wedge tips [i.e., along the x axis—Figs. 1(a) and 1(b)] and coupled across the nanogap by means of the evanescent field in vacuum. It can also be seen that there can exist two different types of coupled plasmon modes in the considered structures. They are characterized by the symmetric and antisymmetric distributions of charges across the gap [Figs. 1(c) and 1(d)]. It can be shown that each of the coupled modes with the symmetric distribution of charges [symmetric coupled wedge plasmons (SCWPs)] has a cutoff separation between the wedges, i.e., they do not exist at arbitrarily small gap width. At a gap width that is less than the cutoff separation, the corresponding SCWP leaks into bulk waves and/or surface plasmons on the sides of the wedges. At the same time, ACWPs do not have a cutoff separation, i.e., they exist at arbitrarily small gap width (in the approximation of continuous electrodynamics). This is similar to the symmetric and antisymmetric plasmons in a vacuum gap separating two identical metallic half-spaces. Therefore, these are ACWPs that form the fundamental mode of a gap plasmon waveguide, and this fundamental mode exists at arbitrarily small gap width.[12] In addition, ACWP is character-

ized by significantly stronger localization near the tips of the wedges, compared to the symmetric modes. Therefore, ACWP is a better candidate for the development of subwavelength plasmonic waveguides.

Sufficiently sharp triangular metal wedges can support more than one wedge plasmon eigenmode.[21] Decreasing wedge angle results in increasing number of wedge plasmon modes supported by the wedge.[21] In the same way, two coupled wedges [Figs. 1(a) and 1(b)] can also support more than one ACWP modes. Decreasing wedge angle results in increasing number of the ACWP modes supported by the wedges (simply because this is the case for each of the coupled wedges separately). Interestingly, decreasing separation between the wedge tips can also result in increasing number of the ACWP modes supported by the structure. This is because decreasing separation between the wedges results in stronger coupling between the wedge plasmons, leading to increasing their wave numbers (see below). This means that the effective permittivity of the guiding structure also increases, which naturally leads to increasing number of guided modes.

Each of the ACWP modes can be investigated separately by the numerical procedure described above. However, in this paper, we will mainly focus on the detailed analysis of the fundamental ACWP mode, because it is the most strongly localized mode and therefore most promising from the viewpoint of design of efficient subwavelength waveguides. At the same time, the major features of the obtained results are also typical for higher ACWP modes.

III. WAVE NUMBERS OF THE FUNDAMENTAL ACWP MODES

It is clear that the major characteristics of the fundamental ACWP modes, e.g., their wave numbers, should strongly depend on various structural parameters, such as wedge angle, roundness of the tips [Fig. 1(b)], dielectric constants of the media in contact, etc. For example, typical dependencies of the wave number k_{ACWP} of the fundamental ACWP mode on radius of curvature r of the wedge tips are presented in Fig. 2 for the silver-vacuum structure with the wedge separation $w=60$ nm.

As expected, at small radii of the tips, the wave number k_{ACWP} decreases with increasing r. This is because increasing radii of the wedge tips results in decreasing their sharpness, leading to weaker localization of the wedge plasmon and smaller wave number. It is clear that at $r\rightarrow+\infty$, the rounded tips tend to form a uniform gap between two flat metallic surfaces. Therefore, at $r\rightarrow+\infty$, k_{ACWP} must tend to the wave number of the gap plasmon, k_{GP}, in the uniform gap of the 60 nm width. This is difficult to achieve numerically, but the tendency demonstrated by all the curves in Fig. 2 confirms this expectation. Another interesting tendency demonstrated by Fig. 2 is that k_{ACWP} decreases noticeably below k_{GP} (dotted line in Fig. 2) as the radius of the tips increases, reaches a minimum at $r=r_m$, and only then increases back to k_{GP}. Increasing angle of the wedges results in a less pronounced minimum of k_{ACWP} (Fig. 2), and the radius r_m at which this minimum is reached decreases with increasing wedge angle ($r_m\approx300$ nm, ≈200 nm and ≈100 nm for $\theta=30°$ 40°, and 80°, respectively). This is because increasing wedge angle results in decreasing typical size (e.g., area) of the rounded tip. Thus the effect of the tip roundness is diminished.

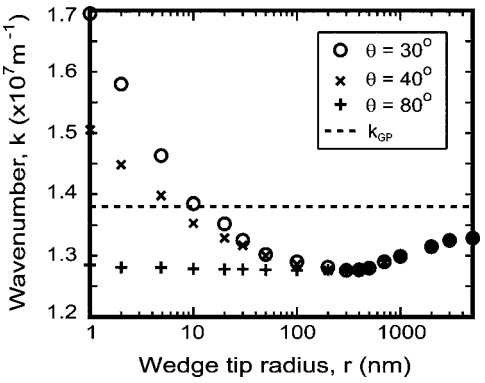

FIG. 2. The dependence of the wave number of the fundamental ACWP mode on radius of the tip for the silver wedges in vacuum at different wedge angles: $\theta=30°$ (○), $\theta=40°$ (×), and $\theta=80°$ (+). Other parameters: gap width is $w=60$ nm, vacuum wavelength $\lambda_{\mathrm{vac}}=632.8$ nm (He–Ne laser), and the corresponding permittivity of silver $\varepsilon_{m1}=-16.2+0.5i$. The horizontal dotted line corresponds to the wave number k_{GP} of the gap plasmon in a uniform gap of the 60 nm width.

All the three dependencies in Fig. 2 tend to merge when the radii of the tips increase above ~200 nm. This is because increasing r results in increasing area of the rounded tips. If the region of ACWP localization is smaller than the typical size of the rounded tips (e.g., the tip radius), then the plasmon does not "feel" the flat sides of the wedges. Therefore, its wave number does not depend on wedge angle (Fig. 2). In this case, we approximately have a localized coupled plasmon propagating between two cylindrical surfaces of radii r, rather than a coupled wedge plasmon. This occurs when the radius of curvature increases above ~200 nm (Fig. 2). On the contrary, if r is small (smaller than ~200 nm in Fig. 2), then the size of the localization region is larger than the size of the rounded tips. Therefore, the ACWP field extends to the flat sides of the wedge and the ACWP wave number depends on wedge angle (increases with decreasing θ—Fig. 2).

The existence of a minimum wave number of ACWP at an "optimal" tip radius r_m is analogous to the existence of a minimum wave number of ACWP at an optimal angle of the triangular wedge (with zero radius of curvature)—see Fig. 3 below. This is because introducing tip roundness at a given wedge angle is similar to increasing angle of the triangular tip—in both the cases, the effective sharpness of the tip is reduced. More detailed physical reasoning of this effect cannot be presented at this stage.

The typical dependencies of the wave numbers of fundamental ACWP mode on wedge angle at zero radius of curvature of the tips [Fig. 1(a)] are presented in Fig. 3 for the silver-vacuum structure at different separations of the tips. In particular, it can be seen that at small wedge angles increasing θ results in a rapid decrease of the ACWP wave number (see also Ref. 21). However, if the separation between the coupled wedges is not too large (so that to produce reasonable coupling), then the ACWP wave number reaches a minimum at an optimal wedge angle [see the stars and empty circles in Fig. 3(a)]. Further increase of the wedge angle results in a monotonous increase of the ACWP wave number

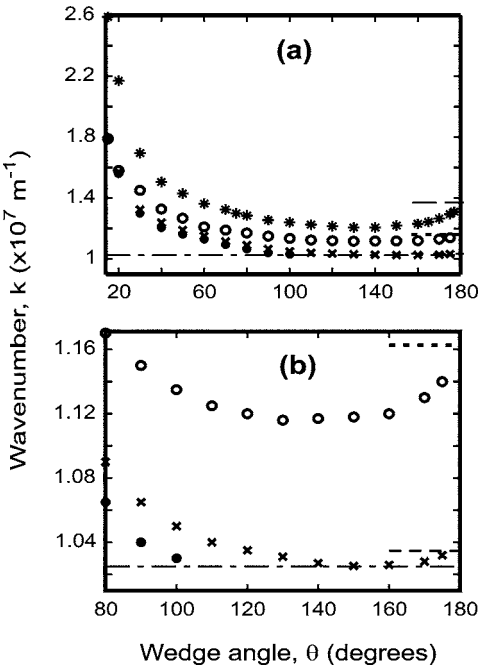

FIG. 3. The dependencies of wave numbers of the fundamental ACWP mode on wedge angle in the structure of two triangular (zero radius of curvature of the tips) coupled silver wedges in vacuum on wedge angle at different separations of the wedges: $w=60$ nm (⋆), $w=150$ nm (○), $w=wc \approx 930$ nm (×), and $w=+\infty$ (●) (an isolated wedge). The straight horizontal lines correspond to the wave numbers k_{GP} of the gap plasmons at the corresponding gap widths: 60 nm (— —), 150 nm (-----), 930 nm (— — —), and k_{SP} of the surface plasmon at an isolated flat surface (— - —), i.e., at the infinite gap width. $\lambda_{vac}=632.8$ nm (He–Ne laser), and $\varepsilon_m=-16.2+0.5i$. Figure 3(b) is the magnification of Fig. 3(a).

to that of the gap plasmon in a uniform gap of the considered separation (when $\theta=180°$ and the coupled wedges form a uniform gap).

As can be seen from Fig. 3, there is a critical separation between the coupled wedges, at which min $\{k_{ACWP}\}$ is equal to the wave number k_{SP} of the surface plasmon (SP) on the isolated metal-vacuum interface. For the triangular silver wedges at $\lambda_{vac}=632.8$ nm the critical separation $w_c \approx 930$ nm, and the wedge angle at which min $\{k_{ACWP}\}=k_{SP}$ is approximately equal to 150° [crosses in Figs. 3(a) and 3(b)]. If $k_{ACWP}=k_{SP}$, this means that the corresponding ACWP is not localized near the tips of the wedges, but is rather formed by four surface plasmons travelling along the sides of the two coupled wedges (with infinite penetration depth along the sides of the wedges). If $w>w_c$, there exists a range of wedge angles $\theta_{c2}<\theta<\theta_{c3}$, within which $k_{ACWP}<k_{SP}$ (the reasons for using indices 2 and 3 in the notations for the critical wedge angles will be clear below). Localized ACWPs as structural eigenmodes can exist only if $\theta<\theta_{c2}$ or $\theta_{c3}<\theta<180°$. Between the second and the third critical angles ($\theta_{c2}<\theta<\theta_{c3}$), ACWPs do not exist as structural eignemodes—they leak into surface plasmons on the sides of the wedges. In the limiting case of infinite separation (isolated uncoupled wedges), the fundamental ACWP mode turns into two separate localized wedge plasmons.[21] In this case, $\theta_{c3}=180°$, and θ_{c2} becomes the upper cutoff angle for the isolated wedge, and if $\theta>\theta_{c2}$, wedge plasmons do not exist as wedge eigenmodes.[21] For an isolated silver wedge in vacuum, the upper cutoff wedge angle $\theta_{c2}\approx 105°$—see Ref. 21 and the dots in Figs. 3(a) and 3(b).

As has been shown in Refs. 24 and 25 strongly localized plasmonic eigenmodes in wedgelike structures, such as metallic V-grooves[24] or triangular wedges,[25] can only exist if the wedge/groove is not too sharp (i.e., its angle θ is larger than the first cutoff angle θ_{c1}). If $\theta<\theta_{c1}$, plasmons in the groove/wedge (including the region near the tip) can be considered in the geometrical optics (adiabatic) approximation. A strongly localized plasmon mode, for example, near the tip of a metal wedge can be represented by two coupled surface plasmons propagating on the two sides of the wedge and successively reflecting from the tip and the turning point (simple caustic).[24,25] If the geometrical optics approximation is satisfied (i.e., $\theta<\theta_{c1}$), then the parameters of these two coupled surface plasmons change only insignificantly within one wavelength (applicability condition for the adiabatic approximation[24,25]). In this case, the coupled surface plasmons do not experience significant reflection as they travel towards the tip, but rather slow down adiabatically and stop asymptotically at the tip (in the approximation of continuous electrodynamics).[24,25] This means that the localization of the corresponding wedge plasmon (or groove plasmon) is infinite, i.e., it does not exist.[24,25] Therefore, θ_{c1} is the lower cutoff angle for the strongly localized wedge plasmons.[25] If $\theta<\theta_{c1}$, the geometrical optics approach (adiabatic approximation) is applicable, and wedge plasmons do not exist, because they are infinitely localized near the tip.[24,25] On the contrary, if $\theta>\theta_{c1}$, the adiabatic approximation is not applicable, and the localized plasmonic modes near the tip of the wedge/groove can exist.[24,25]

As a result, ACWPs can exist only within the ranges of the wedge angles: $\theta_{c1}<\theta<\theta_{c2}$ and $\theta_{c3}<\theta<180°$. Thus, there are three critical angles determining the existence conditions for ACWPs in the structure of two triangular wedges separated by a nanogap. The second and the third critical angles can be determined numerically (see Figs. 3(a) and 3(b)), while the first critical angle is determined from the applicability condition for the adiabatic approximation,[25]

$$\theta_{c1} \approx -2\varepsilon_1/e_1, \tag{1}$$

where ε_1 is the permittivity of the dielectric surrounding the metal wedge, e_1 is the real (negative) part of the metal permittivity, and θ_{c1} is assumed to be small. In the above examples (Figs. 2 and 3), we considered silver wedges in vacuum at $\lambda_{vac}=632.8$ nm, i.e., $\varepsilon_1=1$, $e_1=-16.2$, and the first critical angle $\theta_{c1}\sim 7°$.

At the critical separation w_c between the coupled wedges, $\theta_{c2}=\theta_{c3}$, and the second interval of angles $\theta_{c2}<\theta<\theta_{c3}$, within which ACWPs do not exist, is reduced to just one angle $\theta=\theta_{c2}=\theta_{c3}$. If $w<w_c$, then there exists only one critical angle θ_{c1} and ACWPs can exist in the whole range $\theta_{c1}<\theta<180°$ [Figs. 3(a) and 3(b)].

It is interesting to note that when the wedge angle θ is reduced, the differences between the wave numbers of the fundamental ACWP modes at different separations tend to diminish [compare circles, crosses and dots in Fig. 3(a)]. This is because at any fixed nonzero separation, reducing

wedge angle eventually results in sufficiently strong localization of the plasmon near the tips, so that the penetration depth of the field into the vacuum gap becomes smaller than the gap width. As a result, for any fixed separation between the tips, reducing wedge angle eventually results in decoupling of the wedge plasmons on the two tips, and the wave numbers of ACWPs must thus tend to the wave number of a wedge plasmon on an isolated wedge. Therefore, the stars in Fig. 3(a) must also tend to all other symbols, but at smaller values of θ. This also suggests that the applicability condition for the adiabatic approximation near the tips of the wedges does not depend on separation between them. Therefore, though Eq. (1) was derived near the tip of an isolated wedge,[24,25] rather than for the coupled wedges, it is still correct for ACWPs at arbitrary separation, and its use in the above discussion was justified.

Comparison of the dots with other symbols in Figs. 3(a) and 3(b) also suggests that the wave numbers of the wedge plasmons on an isolated triangular wedge are always smaller than those of the fundamental ACWP modes. This is expected, because the Coulomb attraction between the opposite charges across the gap [Fig. 1(d)] results in decreasing speed and the wavelength of the coupled plasmons (similar to the antisymmetric plasmons in a narrow gap separating two metallic media). This is also a reason why the second critical angle θ_{c2} increases [from $\theta_{c2}\sim 105°$ at $w=+\infty$ to $\theta_{c2}\sim 150°$ at $w=w_c$—Fig. 3(b)] with decreasing separation between the tips. Increasing coupling between the wedge plasmons results in increasing their wave number, thus increasing the range of wedge angles within which the fundamental ACWP mode can exist. The same interpretation can be used for the explanation of the reduction of the third critical angle from $\theta_{c3}\sim 180°$ at $w=+\infty$ to $\theta_{c3}\sim 150°$ at $w=w_c$ [Fig. 3(b)]. Therefore, unlike the first critical angle, the second and the third critical angles are noticeably affected by the coupling between the wedges (i.e., by their separation w).

If the tips of the edges are not triangular, but rounded with a radius of curvature r [Fig. 1(b)], then increasing r results in a decrease of the wave numbers of ACWP fundamental modes at smaller wedge angles. At the same time, when $\theta\rightarrow 180°$, the wave number of the fundamental ACWP mode still tends to the wave number of the corresponding gap plasmon [similar to how it happens in Figs. 3(a) and 3(b)]. This is because, if $\theta\rightarrow 180^{\circ}$, the structure tends to the uniform gap of width w irrespectively of the radius of curvature r of the wedge tips.

Another interesting conclusion is that in the approximation of continuous electrodynamics any nonzero radius of curvature of the wedge tip should result in removal of the first critical angle θ_{c1} (lower cutoff angle). Indeed, an arbitrarily small (but finite) radius of curvature of the tips results in breaching the adiabatic approximation (geometrical optics approximation) near the rounded tip. A plasmon propagating towards the rounded tip will not experience infinite slowing down without any significant reflection (as should be in the adiabatic approximation),[24,25] but rather be reflected from the rounded tip, while still having finite (nonzero) wavelength and noninfinite wave number. This will happen at arbitrarily small wedge angles. As a result, a plasmon guided by the rounded tip of the wedge with finite localization near the tip can exist even if $\theta<\theta_{c1}$. At the same time, decreasing radius of curvature of the rounded tip results in increasing localization of the wedge plasmon. If $\theta<\theta_{c1}$, then decreasing r to zero results in infinite increase of plasmon localization near the tip (i.e., it ceases to exist). If $\theta>\theta_{c1}$, then decreasing r to zero results in only finite increase of the plasmon localization near the tip, the maximal localization will be given by the localization of the wedge plasmon near the triangular tip (i.e., with zero radius of curvature). These arguments are equally relevant to localized plasmons on an isolated metal wedge and all the ACWP modes on two wedges separated by a nanogap.

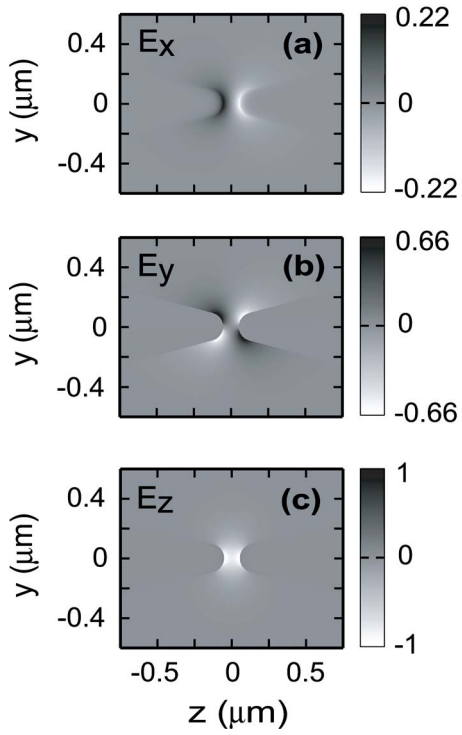

FIG. 4. The distributions of the three components of the electric field near the rounded tips of the couples silver wedges in vacuum; $r=100$ nm, $w=60$ nm, $\theta=30°$, $\lambda_{vac}=632.8$ nm (He–Ne laser), and $\varepsilon_m=-16.2+0.5i$. The electric field components are normalized to $|\max\{E_z\}|$.

IV. FIELD DISTRIBUTION AND PLASMON LOCALIZATION

The typical distributions of the electric and magnetic fields near the rounded tips of the coupled wedges in a cross section that is parallel to the (y,z) plane in the fundamental ACWP mode are presented in Figs. 4 and 5 for all three components of each of the fields. In particular, it can be seen that E_y and H_z are antisymmetric with respect to both the y and z axes [Figs. 4(b) and 5(c)]. E_x is antisymmetric with respect to the y axis and symmetric with respect to the z axis, while H_x displays the opposite symmetry [Figs. 4(a) and 5(a)]. At the same time, the E_z and H_y components are symmetric with respect to both the considered axes. These field distributions are typical for all radii of curvature of the tip including the zero radius (triangular tip), whenever the fundamental ACWP mode exists.

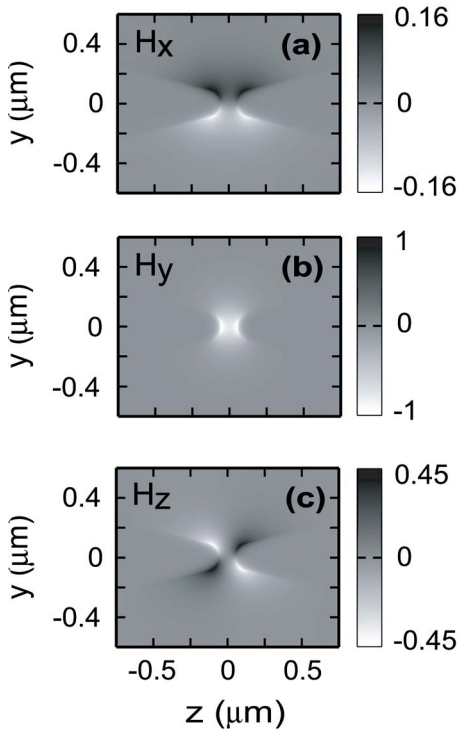

FIG. 5. The distributions of the three components of the magnetic field near the rounded tips of the couples silver wedges in vacuum; $r=100$ nm, $w=60$ nm, $\theta=30°$, $\lambda_{vac}=632.8$ nm (He–Ne laser), and $\varepsilon_m=-16.2+0.52i$. The magnetic field components are normalized to $|\max\{H_y\}|$, $\max\{H_y\}/\max\{E_z\}=9.76\times10^{-4}$ (A/V).

The presented distribution patterns can be understood on the basis of the antisymmetry of the distribution of charges across the gap [Fig. 1(d)]. Indeed, such a charge distribution naturally results in the antisymmetry of E_y and E_x with respect to the y axis [i.e., across the gap—Figs. 4(a) and 4(b)]. Simultaneously, this results in the symmetric distribution of E_z [Fig. 4(c)], caused by the electrostatic interaction between the opposite charges across the gap. The antisymmetry of E_y with respect to the z axis is explained by the fact that wedge plasmon modes are actually guided film plasmons, i.e., two surface plasmons coupled across the film/membrane. In the case of a wedge, the thickness of this membrane (wedge) decreases towards the tip of the wedge. The film plasmon propagates in the structure with varying thickness, which is equivalent to changing effective permittivity for the plasmon.[24,25] There can exist two different film plasmons, those with symmetric and antisymmetric distribution of charges across the film. It can be seen that only the film plasmon with symmetric (with respect to the central plane of the film) distribution of charges does not have a cutoff film thickness. That is, it can exist in the film when its thickness tends to zero, and the wave number of such a film plasmon tends to infinity as the film thickness tends to zero. This is equivalent to increasing effective permittivity for the film plasmon to infinity as the film thickness tends to zero. The film plasmon in a wedge propagates in the structure with changing effective permittivity, i.e., effectively in a waveguide formed by increasing effective permittivity near the tip of the wedge.[24,25] Therefore, the strongly localized wedge plasmon modes are formed by guided film plasmon modes

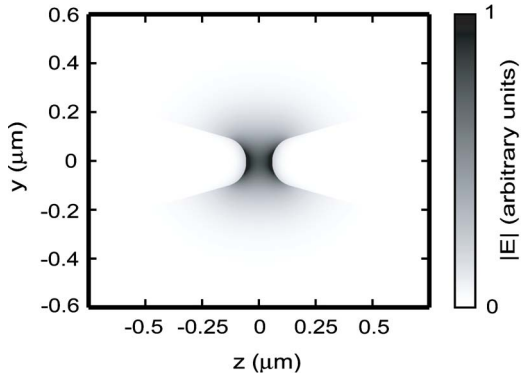

FIG. 6. The distribution of the magnitude of the electric field near the rounded tips of the coupled silver wedges in vacuum; $r=100$ nm, $w=60$ nm, $\theta=30°$, $\lambda_{vac}=632.8$ nm (He–Ne laser), and $\varepsilon_m=-16.2+0.52i$ (silver).

with the symmetric charge distribution across the film.[24,25] The symmetric charge distribution results, for example, in identical positive charges on the opposite sides of a metal wedge near the tip. As a result, these charges will produce identical (in magnitude) electric fields, but pointing in the opposite directions (along the positive and negative y directions). This results in the antisymmetry of E_y and symmetry of E_x with respect to the z axis, which is demonstrated by Figs. 4(a) and 4(b).

The symmetric features of the magnetic field components (Fig. 5) immediately follow from the symmetry of the electric field components (Fig. 4) and the Maxwell equations.

The typical distribution of the magnitude of the total electric field between the tip in the (y,z) plane (perpendicular to the direction of plasmon propagation) is presented in Fig. 6. In particular, it can be seen that the field is primarily localized in the vicinity of the rounded tips in the gap between them. The distribution of the magnitude of the electric field is thus symmetric with respect to both the y and z axes. This immediately follows from the symmetric and antisymmetric distributions of all three electric field components (Fig. 4).

Figures 4–6 suggest strong localization of the ACWP field near and between the wedge tips. In order to investigate the localization of ACWPs in the considered structures more quantitatively, we define the region of localization so that at its boundaries the magnitude of the plasmon field decreases e times compared to the maximal magnitude of the field at the tips. The dependencies of the typical dimensions of this region along the y and z directions for the fundamental ACWP mode on wedge separation at different angles θ are presented in Fig. 7.

In particular, as expected, increasing separation between the wedges and/or wedge angle results in a significant increase of the region of localization (i.e., decrease of localization of the fundamental ACWP mode)—Fig. 7. Localization along the y axis is affected by the wedge angle much stronger, than the localization along the z axis [compare Figs. 7(a) and 7(b)]. This is because the localization along the z axis is mainly determined by the distance between the tips and rapid decay of the field into the metal. At the same time, localiza-

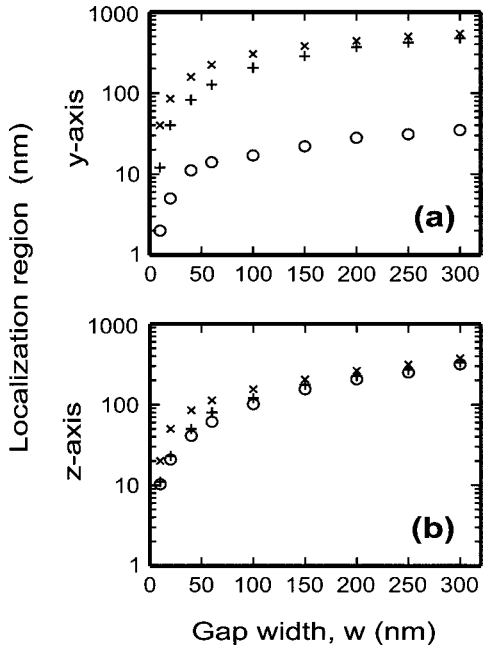

FIG. 7. The dependencies of the dimensions of the region of the field localization (at the level of $1/e$) in the fundamental ACWP mode along the y axis (a) and along the z axis (b) on separation w between the wedges in vacuum. Wedge angles: $\theta=120°$ (×), $\theta=80°$ (+), and $\theta=30°$ (○). The radius of the wedge tips $r=0$, $\lambda_{vac}=632.8$ nm, and $\varepsilon_m=-16.2+0.52i$ (silver).

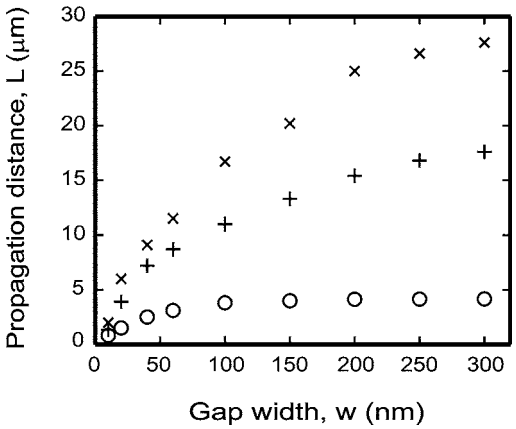

FIG. 8. The dependencies of the propagation distance (the distance at which the field intensity in the fundamental ACWP mode decreases e times) on separation w between the wedges at different wedge angles: $\theta=120°$ (×), $\theta=80°$ (+), and $\theta=30°$ (○). The radius of the wedge tips $r=0$, $\lambda_{vac}=632.8$ nm, and $\varepsilon_m=-16.2+0.52i$ (silver).

tion along the y axis strongly depends on difference between the ACWP wave number and that of the bulk wave in vacuum, and this difference noticeably decreases with increasing separation between the wedges and/or wedge angle (Fig. 2).

As can be seen, the achievable localization of the field between the tips can be far beyond what is called the diffraction limit of light.[3] For example, at $\theta=30°$ and $w=50$ nm, the localization of the fundamental ACWP mode in the considered structure can be as small as ~10 nm (Fig. 7). This makes ACWPs promising from the viewpoint of the development of subwavelength waveguides with strong localization beyond the diffraction limit. Because the fundamental mode of a gap plasmon waveguide is formed by four antisymmetric coupled wedge plasmons,[12] strong localization of ACWPs is also the reason for increasing localization of the fundamental mode in a gap plasmon waveguide with decreasing thickness of the film and/or width of the gap.[12]

V. DISSIPATION OF ACWPS

It is important to understand that strong subwavelength localization of a plasmon is still insufficient for this plasmon to be useful for the development of efficient subwavelength waveguides. Another very important aspect that has to be taken into account is dissipation of the plasmon. If dissipation is large, so that the plasmon hardly propagates a few wavelengths, it cannot be a good option for the development of subwavelength waveguides and interconnectors for integrated optics. For example, this was the case with strongly localized particle plasmons in chains of metallic nanoparticles, where the typical propagation distances do not exceed ~100 nm.[2] Therefore, the numerical analysis of dissipation of ACWP modes is essential for the evaluation of their suitability for the design of efficient subwavelength interconnectors and nano-optical devices.

The typical dependencies of the propagation distances of the fundamental ACWP mode on gap width are presented in Fig. 8 for the structure of two identical silver wedges with zero tip curvature in vacuum. For comparison, the structural parameters are chosen the same as for Fig. 7. For example, at the separation between the wedges of ~50 nm, the propagation distances of the fundamental ACWP mode are between ~2.5 μm (at $\theta=30°$) to ~10 μm (at $\theta=120°$). Taking into account that at $\theta=30°$ the wavelength of the fundamental ACWP mode is ~440 nm (Fig. 3), the propagation distance of ~2.5 μm corresponds to ~ six wavelengths, which is sufficient for the design of interconnectors for nanoscale integrated optics.[1,5] Increasing wedge angle and/or separation between the wedges results in increasing propagation distance and the number of plasmon wavelengths that fit within this propagation distance. However, this will also result in a simultaneous decrease of the localization of the ACWP modes near the tips. Therefore, there should be a reasonable compromise between decreasing propagation distance (increasing dissipation) and increasing localization, as the wedge angle and/or separation between the tips are decreased.

Physically, increasing dissipation with increasing plasmon localization is explained by the fact that the plasmon penetration depth into vacuum rapidly decreases with increasing localization, because the wave becomes increasingly noneigen in the vacuum (dielectric). As a result, a larger portion of the plasmon energy propagates in the dissipative metal, which naturally leads to increasing dissipation of ACWP and decreasing number of wavelengths that the plasmon can travel before the intensity of its field decreases e times. As can be seen from Fig. 8, ACWP propagation distance increases (i.e., dissipation decreases) with increasing separation between the wedges. However, at large values of w, the increasing propagation distance tends to a plateau (see, for example, circle in Fig. 8). This is because at large separations the ACWP fundamental mode tends to two un-

coupled wedge plasmons propagating along the two isolated wedges. Therefore the plateau propagation distances must correspond to propagation distances of the two uncoupled wedge plasmons on isolated wedges.[21]

VI. CONCLUSIONS

In summary, this paper has reported the numerical analysis of strongly localized coupled plasmons propagating along the tips of two metal wedges separated by a nanogap. Plasmon parameters and field structure were determined by means of the compact-2D FDTD formulation. Two types of coupled plasmon eigenmodes can exist in the coupled wedge structure—with the symmetric and antisymmetric distributions of charges across the gap. The symmetric modes have a cutoff separation between the tips of the wedges, while the antisymmetric modes can exist at arbitrarily small separation.

Detailed numerical analysis has been conducted for the ACWP fundamental mode, including its field structure, dispersion, dissipation, existence conditions, typical propagation distances, and the dependencies of the wave parameters on radius of the wedge tips, wedge angle, and separation. It has been demonstrated that the ACWP modes can be used for the design of effective subwavelength waveguides, because their localization can be far beyond the diffraction limit of light, and their dissipation can be relatively weak (so that the wave can normally propagate at least several wavelengths before its intensity drops e times). In particular, decreasing separation between the wedges and/or their angles results in increasing localization of the plasmon near the tips and decreasing their propagation distance. Therefore, separation between the wedges and wedge angle are highly important parameters that should be taken into account when determining the optimal structures for the design of nano-optics components. Further increase of the propagation distances could be achieved by means of gain-assisted propagation (which could be achieved by surrounding the metal wedges by a medium with gain, as was proposed for surface plasmons [26,27]).

The analysis has been conducted primarily for the fundamental ACWP mode. At the same time, the major findings are also applicable for higher ACWP modes in the considered structures (if their existence conditions are satisfied). Similarly, the analysis was conducted only for identical wedges in vacuum coupled across a gap. It is also practically important to consider a structure of two coupled metal wedges on a dielectric substrate. Certainly, the substrate may have a significant effect on the described ACWPs. For example, in some cases, ACWP modes may become leaky into the substrate. This may create an opportunity for a resonant generation of these modes using focused bulk radiation incident onto the structure of the two wedges from the substrate. However, detailed analysis of these effects is beyond the scope of this paper.

ACKNOWLEDGMENTS

The authors gratefully acknowledge support from the Japan Society for the Promotion of Science and the High Performance Computing Division at the Queensland University of Technology.

[1] J. R. Krenn, Nat. Mater. **2**, 210 (2003).
[2] S. A. Maier, P. G. Kik, H. A. Atwater, S. Meltzer, E. Harel, B. E. Koel, and A. A. G. Requicha, Nat. Mater. **2**, 229 (2003).
[3] J. Takahara, S. Yamagishi, H. Taki, A. Morimoto, and T. Kobayashi, Opt. Lett. **22**, 475 (1997).
[4] P. Berini, Phys. Rev. B **63**, 125417 (2001).
[5] J. R. Krenn, B. Lamprecht, H. Ditlbacher, G. Schider, M. Salerno, A. Leitner, and F. R. Aussenegg, Europhys. Lett. **60**, 663 (2002).
[6] C. A. Pfeiffer, E. N. Economou, and K. L. Ngai, Phys. Rev. B **10**, 3038 (1974).
[7] J. R. Krenn, A. Dereux, J. C. Weeber, E. Bourillot, Y. Lacroute, and J. P. Goudonnet, Phys. Rev. Lett. **82**, 2590 (1999).
[8] K. Tananka, M. Tanaka, and T. Sugiyama, Opt. Express **13**, 256 (2005).
[9] B. Wang and G. P. Wang, Appl. Phys. Lett. **85**, 3599 (2004); F. Kusunoki, T. Yotsuya, J. Takahara, and T. Kobayashi, *ibid.* **86**, 211101 (2005).
[10] L. Liu, Z. Han, and S. He, Opt. Express **13**, 6645 (2005).
[11] G. Veronis and S. Fan, Opt. Lett. **30**, 3359 (2005).
[12] D. F. P. Pile *et al.*, Appl. Phys. Lett. **87**, 261114 (2005).
[13] I. V. Novikov and A. A. Maradudin, Phys. Rev. B **66**, 035403 (2002).
[14] D. F. P. Pile and D. K. Gramotnev, Opt. Lett. **29**, 1069 (2004).
[15] D. K. Gramotnev and D. F. P. Pile, Appl. Phys. Lett. **85**, 6323 (2004).
[16] D. F. P. Pile and D. K. Gramotnev, Opt. Lett. **30**, 1186 (2005).
[17] D. F. P. Pile and D. K. Gramotnev, Appl. Phys. Lett. **86**, 161101 (2005).
[18] S. I. Bozhevolnyi, V. S. Volkov, E. Devaux, and T. W. Ebbesen, Phys. Rev. Lett. **95**, 046802 (2005).
[19] T. Yatsui, M. Kourogi, and M. Ohtsu, Appl. Phys. Lett. **79**, 4583 (2001).
[20] A. D. Boardman, G. C. Aers, and R. Teshima, Phys. Rev. B **24**, 5703 (1981).
[21] D. F. P. Pile, T. Ogawa, D. K. Gramotnev, T. Okomoto, M. Haraguchi, M. Fukui, and S. Matsuo, Appl. Phys. Lett. **87**, 061106 (2005).
[22] D. F. P. Pile, Appl. Phys. B: Lasers Opt. **81**, 607 (2005).
[23] G. Mur, IEEE Trans. Electromagn. Compat. **40**, 100 (1998).
[24] D. K. Gramotnev, J. Appl. Phys. **98**, 104302 (2005).
[25] D. K. Gramotnev and K. C. Vernon (unpublished).
[26] M. P. Nazhad, K. Tetz, and Y. Fainman, Opt. Express **12**, 4072 (2004).
[27] S. Maier, Opt. Commun. **258**, 295 (2006).